

that that the motions of borders of zigzag walls are strongly correlated.^{19,20}

In this paper, results of both experimental and theoretical investigations of chevroned samples SSFLCs are reported with the aim of explaining the effect of field-induced excitations of the zigzag defects on the dynamic behavior of the considered systems over all their dynamic phases. It is clear that mechanisms responsible for the appearance of dynamic phases in defected SSFLCs are different and, in general, more complex than those occurring in solid-state media with domain structures. Nevertheless, results presented here yield insight into dynamic phase transitions and properties of dynamic phases in disordered systems. In particular, it is shown that processes of sliding of defect walls can convert systems into different dynamic states. As an experimental method, the electro-optic technique supported by microscopic observations was applied. This technique enabled one to register the electro-optic response of small fragments of samples and thereby enabled one to analyze the contribution to the electro-optic response coming from collective motions of molecules within the zigzag defects. The chosen systems were thin samples of ferroelectric liquid-crystalline mixtures: Felix 15–100 and Felix 17–100. Molecules forming these mixtures display large shape anisotropy, low symmetry, and strong polarity. In thin cells, the molecules are preferentially arranged in liquidlike (smectic) layers and the whole samples exhibit ferroelectric ordering under surface interactions.³ At sufficiently high temperatures and/or in cases of cells of sufficiently small thicknesses, the smectic layers are oriented perpendicularly to boundary plates. However, when the cell thickness is not very small, the smectic layers narrow and spontaneously bend at a rather small angle to boundary plates as temperature is lowered. As a result, a chevron structure of smectic layers arise which, typically, is not perfect but contains zigzag defects.

II. RELAXATION MOTIONS OF DEFECTS

Molecular motions studied here were induced by applying normally to boundary plates of samples a sinusoidally oscillating voltage $V(t) = U \sin(\omega t)$ where U denotes the rms amplitude and $\omega = 2\pi f$ with f being the frequency. As it is well known, collective rotations of molecules driven by weak voltages can easily be detected by measuring the electro-optic response of liquid-crystal systems. In addition to contributions due to collective rotations of molecules within chevron layers, the dispersion of the dielectric permittivity of SSFLCs exhibits a distinct broadband contribution at weak, relatively low-frequency voltages.¹⁹ This is exemplified in Fig. 1, where a contour map showing the U and f dependences of an experimentally determined dielectric loss permittivity ϵ'' is drawn in the case of a cell filled with the Felix 15–100 mixture. For this system, the low-frequency band is visible for $U < 0.5$ V, covering roughly the frequency range $10 \text{ Hz} < f < 1 \text{ kHz}$. It has been suggested that such a low-frequency contribution to the dielectric spectra $\epsilon(\omega)$ is due to oscillatory motions of molecules within zigzag defects.^{20,21} This suggestion can be supported by analyzing electro-optic response recorded for particular sample fragments. The U

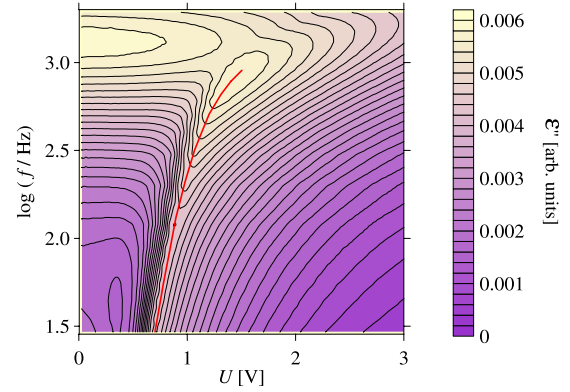


FIG. 1. (Color online) Semilog plot of the contour graph of the dielectric loss $\epsilon''(f, U)$ determined experimentally at the temperature $T=50$ °C, for a cell of the thickness $5 \mu\text{m}$, containing the Felix 15–100 mixture. The solid red line indicates the location of a projection of an edge line of $\epsilon''(f, U)$ on the U - f plane (see Sec. III).

dependence of ϵ'' measured by illuminating very small areas of a sample, the one containing a thick wall and the other having entirely undefected chevron structure, is presented in Fig. 2. It is seen from the figure that, at weak voltages, a relatively low-frequency band occurs in the presence of zigzag defects, and does not appear when these defects are absent. Further arguments for special importance of zigzag walls to dynamic properties of chevron SSFLCs are afforded by microscopic observations. An exemplary micrograph of zigzag walls at zero voltage is shown in Fig. 3 where strips of different colors inside these walls are easily visible. Such diversity of colors of different regions within defect walls is associated with an inhomogeneity of the distribution of the tilt angle of molecules over zigzag walls (especially over thick walls) caused by the influence of borders of the walls. Consequently, one can expect that borders of the zigzag walls strongly disturb field-driven collective rotations of molecules inside zigzag walls affecting the electro-optic response of whole systems. As already been shown,¹⁹ dielectric

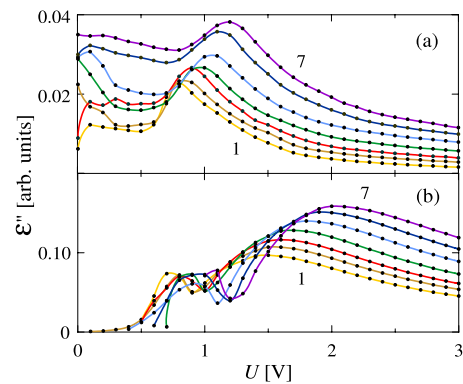


FIG. 2. (Color online) The dielectric loss ϵ'' vs U registered (filled circles) for a Felix 15–100 mixture sample of the thickness $5 \mu\text{m}$ at $T=50$ °C and at $f=70$ (1), 110 (2), 150 (3), 220 (4), 320 (5), 420 (6), and 520 Hz (7). The measurement data were performed for sample fragments with zigzag walls (a) and without these defects (b).

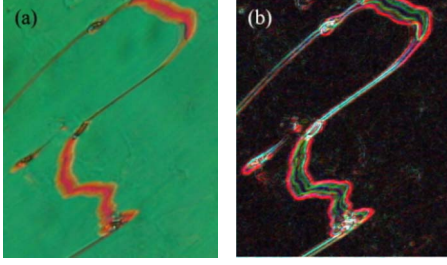


FIG. 3. (Color online) (a) Micrograph of zigzag walls in a Felix 17–100 mixture sample of the thickness $4.63 \mu\text{m}$ taken at $T=50 \text{ }^\circ\text{C}$ and $U=0$. (b) The same micrograph with enhanced contrast. The effect of the variation of the color across wall strips is a clear demonstration of an alternation of the molecular tilt angle across the walls, especially across the thick walls.

spectra of chevron samples contain a broad low-frequency component. On the other hand, dielectric spectra of regular (undefected) SSFLCs with the chevron structure have been determined theoretically. It proves that the subtraction from experimental spectra $\varepsilon(\omega)$ corresponding dielectric spectra derived theoretically has yielded a pronounced frequency dependence of the resulting extracted spectra over a rather wide range of relatively low frequencies.¹⁹ These extracted spectra have been well fitted with spectra determined for Debye processes with a distribution $g(\tau) \sim \tau^{-2}$ of the relaxation time τ .

In order to verify the hypothesis that dielectric spectra corresponding to relaxation motions of molecules within zigzag walls can be described by spectra of Debye processes with continuously distributed relaxation times, consider the equation of motion molecules in the chevron plane. The sample geometry is taken here to be identical to that of Refs. 19 and 20, where the smectic layers are parallel to the (X - Z) plane, the boundary plates of the sample are perpendicular to X axis and the origin of the coordinate frame is placed in the chevron interface plane at the border between the chevron region and a given thick wall. For simplicity, the wall is assumed to spread out along the Z axis. The rotation motion of molecules within the wall can be investigated in the continuous approximation by analyzing field-induced fluctuations of the azimuthal angle $\phi = \phi(x, z)$, characterizing the orientation of the c director within planes parallel to the (X - Y) plane both along the X and Z axes. Since borders of samples used in experiments have rigidly been glued and distances between boundary plates have been kept constant by hard spacers, piezoelectric effects²² have not been observed. Therefore, in the description of the studied systems, these effects can be neglected especially in cases of low applied fields. Consequently, in the presence of an electric field, applied along the X axis and sinusoidally alternating with the frequency ω , the rotational motion of molecules forming defects is described by the equation

$$M \frac{\partial^2 \phi}{\partial z^2} + K \frac{\partial^2 \phi}{\partial x^2} - \gamma \frac{\partial \phi}{\partial t} = G \sin \phi \cos \omega t, \quad (1)$$

where M and K ($M \ll K$) are respectively interlayer and intra-layer twist interactions, γ is the rotational viscosity, and $G = P_s U / d$ with P_s denoting the local polarization and with d

being the cell thickness. The surface anchoring interactions are assumed here to be strong compared with the K coupling and the sample is assumed to be very thin. Under these assumptions, the dependence of ϕ on x is weak for low voltages and the rotational viscosity can then be treated as independent of x . However, the borders between chevron and bookshelf (defect) layers can affect the azimuthal angle through interlayer couplings, even far away from the boundaries (as seen in Fig. 3). Accordingly, the rotational viscosity cannot be treated within defect walls as a constant, i.e., $\gamma = \gamma(z)$. The resulting dependences of ϕ and thereby γ on z will be assumed here to persist through a distance L from the wall border less than half a width of a defect wall. In general, the borders between defect walls and their chevroned surroundings have rather complex structures.³ However, the slope of chevron smectic layers (in the chevron plane) is usually small and the borders can be treated as simple connection of chevron and bookshelf smectic layers (in the case of thick walls such as connection can schematically be presented as $\dots \rangle \rangle \langle \langle \dots$). Then, the solution of Eq. (1) can be written for low voltages and for $0 \leq z \leq L$ in the form

$$\phi(x, z; t) = g(x, z) - B(x, z) \sin[g(x, z)] \cos \beta \cos(\omega t - \beta) \quad (2)$$

with

$$g(x, z) = \phi_0 + bx + c \left(1 - \frac{z}{L} \right), \quad (3)$$

$$B(x, z) = \frac{G}{Kb^2 + MH(x, z)}, \quad (4)$$

$$H(x, z) = \left(\frac{c}{L} \right)^2 + \frac{2c}{L} \cot[g(x, z)] h^{-1} \frac{\partial}{\partial z} h - h^{-1} \frac{\partial^2}{\partial z^2} h, \quad (5)$$

where $h = (\cos \beta)^2$ and the phase $\beta = \beta(x, z)$ is given by the relation

$$\tan \beta(x, z) = B(x, z) \gamma(z) \omega / G. \quad (6)$$

The constants ϕ_0 and b can be determined using boundary conditions for a given $0 \leq z \leq L$ and $U=0$. For $z=L$, one has $\phi_0 = (\phi_b + \phi_t) / 2$ and $b = (\phi_t - \phi_b) / d$, where ϕ_b and ϕ_t are zero-field values which ϕ takes for $z=L$ at top and bottom sample plates, respectively. In turn, ϕ_b and ϕ_t are related to surface anchoring energy strengths^{23,24} through the following implicit equation

$$\gamma_1 [\sin(2\phi_b) + \sin(2\phi_t)] = \gamma_2 (\sin \phi_t - \sin \phi_b), \quad (7)$$

where γ_1 and γ_2 are respectively the nonpolar and polar surface energy strengths. Clearly, the factor c characterizing the strength of inhomogeneity of the molecular orientation in the z direction depends on the interlayer coupling M .

The local relaxation time is obtained using Eqs. (4)–(6)

$$\tau(x, z) = \frac{\gamma(z)}{Kb^2 + MH(x, z)}. \quad (8)$$

This relation indicates that the influence of borders of the zigzag walls on the rotational motion of molecules forming zigzag walls leads to the space dependence of local relaxation time both in the z and x directions. However, since $K \gg M$, $\tau(x, z)$ can be approximated by

$$\tau(z) \approx \frac{\gamma(z)}{Kb^2}. \quad (9)$$

Within this approximation, τ is identical inside each smectic layer but being dependent on z , τ still have a local character. To determine z dependences of τ and γ , let us consider the field-induced deviation of $\phi(x, z, t)$ from its zero-field form averaged along the x direction and during time period of one cycle of the electric field $\overline{\Delta\phi} = \sqrt{\langle (\Delta\phi)^2 \rangle_{x,t}}$, where $\Delta\phi = \phi(x, z, t) - g(x, z)$ and $\langle \dots \rangle_{x,t} = \int_0^{1/f} (d^{-1} \int_{-d/2}^{d/2} \dots dx) dt$. Using Eqs. (2) and (3), one obtains for $bd \ll 1$ and small enough $|c|$

$$\overline{\Delta\phi} = \frac{1}{2} \tilde{B} \sin^2 \phi_0 \cos \beta(z), \quad (10)$$

where $\tilde{B} = G/Kb^2$ and $\beta(z)$ is given by the relation

$$\tan \beta(z) = \tilde{B} \gamma(z) \omega / G. \quad (11)$$

In the case of small $|c|$, $\overline{\Delta\phi}$ may be estimated as

$$\overline{\Delta\phi} \sim 1 - a + a \frac{z}{\ell(\omega)}, \quad (12)$$

where a is a constant such that $0 < a < 1$, and $\ell(\omega)$ is the distance through which the influence of the wall border on the field-induced contribution to the azimuthal angle is significant. (For a given voltage amplitude, ℓ depends only on ω .) Applying Eqs. (10)–(12), one can easily find the functions $\tau(z)$ and $\gamma(z)$. Since the main low-frequency contributions to the dielectric spectra are expected to come from defect regions close to their borders with chevron smectic layers, these functions can be approximated for sufficiently large a and $\omega\tau(z) > 1$ by

$$\tau(z) \approx \frac{\tau_1}{1 - a + a \frac{z}{\ell(\omega)}}, \quad (13)$$

and

$$\gamma(z) \approx \frac{\gamma_1}{\tau_1} \tau(z), \quad (14)$$

where τ_1 and γ_1 are the bulk values which $\tau(z)$ and $\gamma(z)$ take, respectively, for $z > \ell(\omega)$, i.e., in bookshelf regions that are not influenced by the borders.

In order to calculate the dielectric response due to relaxation processes within zigzag walls, let us make the same assumptions that led to Eq. (13), i.e., $K \gg M$ and $|c| \ll 1$. Under these conditions

$$\phi(x, z; t) = \phi_0 + bx - \tilde{B} \sin(\phi_0 + bx) \cos \beta(z) \cos[\omega t - \beta(z)], \quad (15)$$

where $\beta(z)$ is given by $\tan \beta(z) = \omega\tau(z)$. Using this relation and assuming that $bd \ll 1$ yields the local (z dependent) contribution to the dielectric spectra owing to molecular rotations of molecules within a zigzag wall at the distance $z \leq \ell(\omega)$ from the border of the wall. As can be expected, these spectra have the Debye-type form

$$\Delta\varepsilon^*(\omega; z) = \frac{\Delta\varepsilon(0)}{1 + i\omega\tau(z)} \quad (16)$$

with $\varepsilon(0) = \tilde{B}d^2 \sin^2 \phi_0 / U$. Total dielectric spectra associated with molecules placed inside defects over the distance $\ell(\omega)$ from borders of the defects can be expressed as

$$\Delta\varepsilon^*(\omega) \sim \int_0^{\ell(\omega)} \Delta\varepsilon^*(\omega, z) dz. \quad (17)$$

Note that the proportionality constant between $\Delta\varepsilon^*(\omega)$ and the integral of the above relation should involve the density of defects. According to Eq. (13), one has

$$\Delta\varepsilon^*(\omega) \sim \frac{\ell(\omega)\tau_2}{a} \int_{\tau_1}^{\tau_2} \frac{d\tau}{\tau^2(1 + i\omega\tau)}, \quad (18)$$

where $\tau_2 = \tau_1 / (1 - a)$ is the value of $\tau(z)$ at $z = 0$. The frequency dependence of $\ell(\omega)$ (keeping the voltage amplitude constant) can be determined by balancing the elastic and the viscous (dissipation) energies as well as the energy of interactions of molecules with the external electric field. This leads to the following relation for time averages of the respective energy densities

$$\langle M \phi_{zz} \dot{\phi} - \gamma \dot{\phi}^2 \rangle_{z,x,t} = \langle G \sin(\phi_0 + bx) \cos(\omega t) \dot{\phi} \rangle_{z,x,t}, \quad (19)$$

where $\phi_{zz} = \frac{\partial^2}{\partial z^2} \phi(x, z, t)$, $\dot{\phi} = \frac{\partial}{\partial t} \phi(x, z, t)$, and the average $\langle \dots \rangle_{z,x,t} = \ell^{-1}(\omega) \int_0^{\ell(\omega)} \langle \dots \rangle_{x,t} dz$. Note that the elastic energy associated with the interaction K does not give any contribution to Eq. (19) as $\langle \phi \dot{\phi} \rangle_t = 0$. Calculating the averages in Eq. (19) with the use of Eqs. (13)–(15) and under the assumption that $bd \ll 1$ yields for $\omega\tau_1 > 1$

$$\ell(\omega) \approx \frac{\eta}{\omega}, \quad (20)$$

where

$$\eta = a\tilde{B} \sqrt{\frac{2M}{\tau_1(\gamma_1 + G\tau_1)}}. \quad (21)$$

Thus, the contribution of field-stimulated rotational relaxation motions of molecules within defects to the dielectric response of a chevroned sample can approximately be described by a spectrum of Debye processes with continuously distributed relaxation times. Then,

$$\Delta\varepsilon^*(\omega) = \int_{\tau_1}^{\tau_2} \rho(\omega, \tau) \frac{d\tau}{1 + i\omega\tau}, \quad (22)$$

with the distribution of relaxation times

$$\rho(\omega, \tau) \sim \frac{1}{\omega\tau^2}. \quad (23)$$

This analytical expression for the distribution of relaxation times reproduces the earlier result deduced from experimental data.¹⁹ The limit relaxation times τ_1 and τ_2 given in Ref. 19 have been adjusted by fitting $\Delta\varepsilon^*(\omega)$ of the form (22) to measurement data on dielectric relaxation in samples of various thicknesses. It is remarkable that the relaxation time τ_1 in bulk-bookshelf smectic layers forming defects is nearly half of the relaxation time $\tau_{\max} = 1/\omega_{\max}$, where ω_{\max} is the field frequency at which collective molecular rotations within bulk-chevron smectic layers give the maximal contribution to the dielectric loss spectra.¹⁹ This is in accordance with both theoretical and experimental results that the relaxation time corresponding to collective rotations in liquid crystals in thin cells is proportional to the cell thickness.¹⁹ Note that the thickness (along the Z axis) of bookshelf smectic layers is nearly twice as large as the thickness of each of the chevron slabs (the chevron tilt angle is usually small).

The above results show the importance of relaxation processes within defect walls (especially inside thick zigzag walls) for the electro-optic response of SSFLCs at low frequencies of the driving field. It is clear that the chevron environment of defect walls being perturbed by these defects also gives a contribution to low-frequency dielectric spectra. However, the bookshelf smectic layers forming defects as being a remnant of the high-temperature phase are much less stable and thereby much more field-sensitive than the chevron smectic layers. Therefore, the influence of relaxational processes within chevron smectic layers located near defect borders on low-frequency spectra is considerably weaker than similar processes in defect walls.

III. CREEP DYNAMICS

Field-induced rotational excitations of molecules within zigzag walls become strongly nonlinear in the regime of relatively low frequencies when the voltage amplitude approaches from below a frequency-dependent threshold $U_c(f)$ as seen in Fig. 1. The growth of the dielectric loss in this frequency regime for increasing U , distinctly exemplified in Figs. 1 and 4, indicates that the molecular excitations still remain collective as $U \nearrow U_c(f)$, although they become increasingly nonlinear. As soon as U exceeds for a given f , the threshold $U_c(f)$, the dielectric loss abruptly diminishes (see Fig. 4). This suggests that rotations of molecules forming defect walls lose their collective character for $U > U_c(f)$ (and for relatively small f) leading to the destabilization of smectic layers at borders of the walls and causing viscous creep motions of these walls. Such space confined wall motions are associated with sequences of local restructuring of smectic layers, which can schematically be represented as $|| \rightarrow \rangle\rangle$ and/or $\rangle\rangle \rightarrow ||$. Indeed, the creep motions of thick zigzag walls

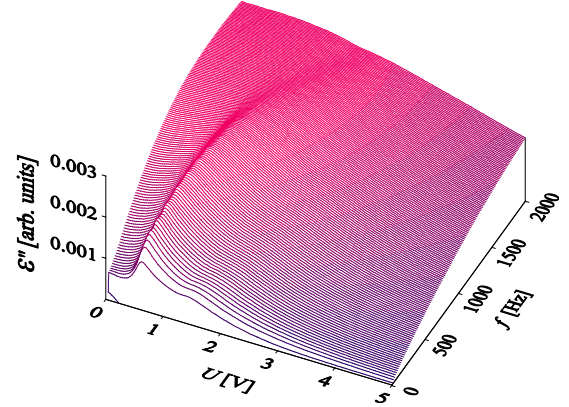


FIG. 4. (Color online) Dependence of the dielectric loss ε'' on U and f experimentally determined at $T=50$ °C for a sample of the thickness 4.63 μm , filled with the Felix 17–100 mixture.

have been observed by means of the polarizing optical microscope at somewhat greater values of U than $U_c(f)$, when these motions irregularly spread over sufficiently large sample regions (much less, however, than whole samples).^{19,20} These observations have given an evidence that the spatial confinement of creeping of the thick walls is a result of a strong pinning of their ends by thin zigzag walls. Additionally, the roughening of borders of thick zigzag walls have been registered (at least in macroscopically large length scales) and a strong correlation between motions of both borders of each of the thick walls has been noticed. The consistency of irregular motions (roughening processes) of both wall borders is a sign of the great importance of interlayer interactions within thick walls to their creep dynamics.

The dynamic transition between relaxational and creep dynamic phase is plainly visible in the occurrence of a narrow convex edge of the surface describing the dependence of the dielectric loss on U and f as shown in Fig. 4. The projection of this edge on the U – f plane defines for a range of rather low frequencies, a critical line $U_c(f)$ (the red line exemplified in Fig. 1). Above the upper cutoff frequency, the oscillations of applied voltage are too fast in order to creep motions could be excited. In turn, at very low frequencies (typically below 10 Hz), even the electro-optic technique is unable to detect slow creep motions of defect walls in a consequence of strong perturbations of the dielectric spectra by ionic currents and by electrode blocking processes.^{21,25,26} For several samples of different thicknesses and filled with different liquid-crystal mixtures, the critical line has been shown to satisfy a scaling relationship, $U_c(f) \sim f^\alpha$ with $\alpha = 0.5 \pm 0.05$.²⁰ The question whether the critical index α is universal (for SSFLCs with the chevron structure) remains, however, open. It should be noted that the discussed dynamic phase transition is also reflected in the U dependence of the dynamical hysteresis-loop area experimentally determined for relatively low frequencies.²⁰ As a consequence, one recovers the scaling form of $U_c(f)$.

The mechanisms underlying relaxation and viscous creep motions in chevroned liquid crystals are very different. While the first kind of motion consists in molecular oscillatory rotations (in both chevron and bookshelf smectic layers)

without changing the structure of samples, the second type of motion relies on restructuring of chevron smectic layers into bookshelf ones or conversely. This is in contrast to similar transitions occurring in solid-state multidomain systems in which segmental relaxation excitations and creep motions of domain walls both consist in local switching processes. Therefore, the relaxation-to-creep transition influences the dielectric response spectra much more distinctly for the chevron SSFLCs than for the solid-state systems.^{6,12}

As the voltage amplitude continuously increases within the creep regime, thick zigzag walls gradually lose their stability and transform themselves into creeping thin zigzag walls. Direct observations have indicated that this field-provoked conversion of the thick walls into the thin ones is accomplished by progressive roughening of the thick walls. During such a process, both interfaces bounding a given thick wall consistently evolve from rather smooth surfaces to very rugged surfaces.²⁰ As a result, interfacial instabilities lead to an emergence from each thick wall growing and simultaneously narrowing kinked stripes, which ultimately constitute (3D) thin walls immediately undergoing localized creep motions.

IV. SLIDE MOTIONS

Sliding viscous motions of zigzag walls (without crossing each other) appear at rather high applied voltages as their amplitude exceeds a frequency-dependent threshold. According to the scenario found in Felix 15–100 mixture systems, after the degradation of thick walls, the motion of thin walls changes under the growing voltage from localized creeping to large-scale (ergodic) slidings, which ultimately cause the walls to move away from samples.¹⁹ Since, in the sliding regime, the thin walls move across cells and vanish at cell boundaries, the density of the walls decreases in time.

It turns out, however, that yet another scenario of sliding motions takes place, e.g., in the case of thin samples containing the Felix 17–100 mixture. In these samples, sliding movements of thin walls are also preceded by a transformation of thick walls into thin walls but the latter are not successively swept off samples, even for voltage amplitudes much greater than the sliding threshold value. Furthermore, the thin walls invade chevron regions when the voltage amplitude exceeds a frequency-dependent threshold value until the whole samples are fulfilled by the walls. To illustrate this process, microphotographs of a fragment of a sample filled with the Felix 17–100 mixture have been presented in Fig. 5, where thin walls at different creep dynamic states (a), (b), and (c) as well as at the sliding invasion process (d) are shown. Such an invasion process resembles both viscous fingering with side branching (especially, the field-induced fingering observed in antiferroelectric liquid crystals)²⁷ and sliding motions. However, in contrast to invading viscous fingers occurring in antiferroelectric liquid crystals, defects migrating into chevron regions of considered systems are not moving fronts of wedgelike domains but remain thin walls with strongly correlated bounding interfaces. Thus, large-scale invading movements of thin zigzag walls can be treated as invading slide motions.

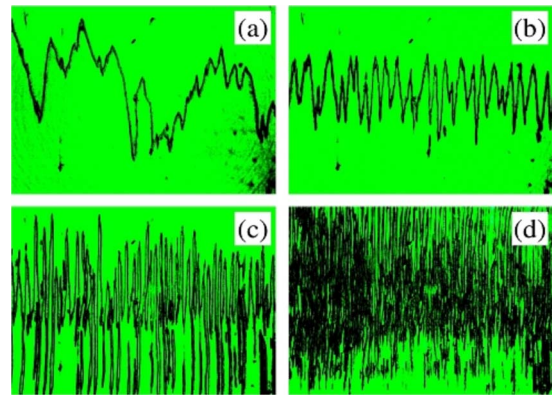


FIG. 5. (Color online) Microphotographs of thin walls in a cell of the thickness $4.63 \mu\text{m}$ filled with the Felix 17–100 mixture at $T=30^\circ\text{C}$, $f=1000 \text{ Hz}$, and different values of U : 8 (a), 12 (b), 16 (c), and 18 V (d). The micrographs (a), (b), and (c) were taken in the regime of the thin-wall creeping, while the micrograph (d) was taken slightly above the sliding threshold value of the voltage amplitude, during the process of the slide invasion of defect walls.

Both types of slide wall motions registered in different SSFLCs of the chevron structure at strong enough driving fields, i.e., rather smooth movements that lead to the disappearance of the walls after reaching system boundaries and invasion movements of walls over whole samples involve restructuring and rearrangement phenomena at interfaces between bookshelf and chevron smectic layers. At strong fields, these phenomena have to a great extent noncollective character. That is the reason why the considered sliding motions similarly to creep motions at high fields do not yield appreciable contributions to dielectric response spectra (see Fig. 1), in order to these motions could experimentally be registered using the electro-optic technique. Consequently, the field-induced transition between creep and sliding dynamic phases is not reflected in electro-optic response spectra as well. One can infer, however, that this transition is smeared at nonzero temperatures similarly to the creep-to-slide transition in various disordered media.⁴ This can mainly originate in inhomogeneities of the layer anchoring at cell plates.

The occurrence of sliding motions of a given kind in chevron SSFLCs is determined by an interplay of the rotational viscosity as well as intralayer and interlayer twist interactions within defect walls on the one hand and within chevron system regions on the other hand. In particular, the invading slide motions are expected to appear when the rotational viscosity of molecules forming zigzag walls is considerably smaller than the viscosity of molecules in chevron smectic layers. It is remarkable that the slide motions of both types have been observed in a wide range of voltage frequencies including low frequencies (for appropriately large voltage amplitudes).

V. SWITCHING DYNAMIC MODES

Field-induced switching between bistable orientational states of molecules in chevron and bookshelf smectic layers proceeds in different ways.^{24,28} Hence, the polarization

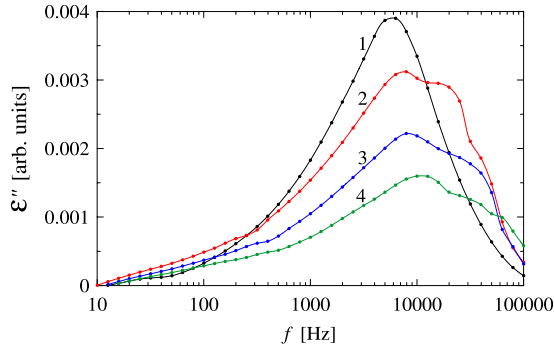


FIG. 6. (Color online) Dielectric-loss spectra experimentally obtained (filled circles) for a Felix 15–100 mixture sample of the thickness 5 μm at $T=50$ $^{\circ}\text{C}$ and at different voltage amplitudes: 10 (1), 60 (2), 80 (3), and 100 V (4).

switching processes within regular and defect regions of the considered systems should, in general, begin to occur at different threshold values of the voltage amplitude (at a given voltage frequency). Generally, these processes are expected to appear at high voltages (much higher than the sliding threshold). However, in that case, the effect of straightening of chevron layers (diminishing the angle of the tilt of the chevron layers) is very strong³ and then the difference in structure between chevron and bookshelf layers vanishes. Consequently at very high voltages, the considered systems can be approximately treated as homogeneous (undefected) bookshelf systems. Then, taking into account nonlinear effects, important at high voltages, e.g., depolarization,^{29,30} and/or nonpolar anchoring of smectic layers at boundary sample plates,³¹ one gets the following equation describing rotational motions of molecules in the considered systems under strong alternating electric field³⁰

$$K \frac{\partial^2 \phi}{\partial x^2} - \gamma \frac{\partial \phi}{\partial t} = G \sin \phi (\cos \omega t - G' \cos \phi), \quad (24)$$

where G' is a constant. As it is known, this equation has a soliton-type solution.³⁰ Accordingly, switching processes in SSFLCs can be performed through oscillatory motions of orientational kinks on the distance $\zeta \sim 1/\omega$ (in the direction perpendicular to sample plates) with the velocity $v = v_0 \cos \omega t$, where v_0 is a constant. Such solitonlike excitations are possible for sufficiently large voltage frequencies when the sample thickness d is much greater than ζ . These excitations have experimentally been registered by measuring the electro-optic response of ultrathin samples with the bookshelf structure at large voltage frequencies.³² It has also been shown that the switching of polarization of these samples as a whole takes place during each cycle of the driving voltage in the regime of low frequencies and very high voltage amplitudes (greater than those at which soliton waves begin to be excited).³²

To study the switching dynamics of the considered systems, their electro-optic response has been measured over a wide range of voltage amplitudes. Results obtained for the dielectric loss spectra are illustrated in Fig. 6. These spectra exhibit a distinct high-frequency band with the peak fre-

quency located between 5 and 10 KHz, for $10 \text{ V} \leq U \leq 100 \text{ V}$. Such a high-frequency band of the electro-optic response occurring at large applied voltages can be affected by solitary switching waves.³² Another broadband appears in ϵ'' at low frequencies, when U is sufficiently large. In Fig. 6, the low-frequency band is visible for $U \geq 50 \text{ V}$, within the frequency range $10 \text{ Hz} \leq f \leq 500 \text{ Hz}$. Clearly, this frequency band of ϵ'' occurring at very high voltages can be attributed to complete polarization switching processes, each of which takes place during one voltage cycle.³² It is remarkable that the low-frequency band shown in Fig. 6 is not very pronounced and, even, reveals a tendency to vanish as U grows. This can be explained that strong electrohydrodynamic convection appearing at very high voltages strongly disturbs coherent rotational molecular motions forced by applied voltages.³³ It should be noted that electroconvection patterns have really been observed in the studied samples within the regime of small frequencies and large voltage amplitudes ($U \geq 50 \text{ V}$).

The transition from sliding to switching dynamic modes in chevron SSFLCs as U increases is followed by processes of straightening of chevroned smectic layers. Thus, the difference between zigzag walls and their chevroned environment is very subtle at large U and this transition has not a sharp character. Since the sliding motions of zigzag walls appear within wide frequency ranges (these defect motions were observed in Felix 17–100 mixture samples even above 5 kHz), the transition to the switching dynamic mode can proceed in two different manners depending on the frequency of the driving voltage. For low frequencies, the transition to the complete switching mode is expected while at sufficiently high frequencies, the appearance of the soliton-like dynamic mode is more probable.

VI. CONCLUSIONS

Dynamic modes of zigzag defect walls in chevron SSFLCs have been shown to differ essentially from those studied in the context of domain walls in ferroic systems. Although the relaxation response spectra induced by weak fields have polydispersive character in both types of systems, they have very different origin. While the low-frequency relaxational dynamic mode in ferroics is associated with segmental oscillations of domain walls (on the length scales less than the sample thickness), the low-frequency relaxation band of the response spectra in chevron SSFLCs appear to be attributed to small rotational motions of molecules forming zigzag defects. In particular, it has been argued that an intricate low-frequency contribution to the dielectric response of the studied systems on weak applied voltages results from the inhomogeneity of rotational viscosity inside defect walls, due to the influence of wall borders on the dynamic behavior of molecules forming the defect walls. The response of zigzag walls theoretically obtained for the relaxation regimen has been proved to be consistent with earlier experimental data. In contrast to result obtained for ferroic systems, the relaxation spectra of the zigzag walls cannot be described by a broadened Debye-type function with an averaged relaxation time. The transition between relaxation and creep

phases has been found to be sharp as the voltage amplitude grows. Direct microscopic observations have indicated that creep motions of the zigzag walls proceed in two stages as the voltage amplitude increases. At the first stage, creep motions of thick walls are excited. These motions are localized, owing to the strong pinning of the ends of thick walls by the thin walls. At the second stage, the thick walls are transformed into the thin ones, which simultaneously start to creep. In addition to sliding dynamic mode involving delocalized defect motions without increasing in time the space average of wall lengths, a new type of sliding movements the so-called invading slide mode has been observed. This dynamic mode is associated with the elongation and side branching of thin zigzag walls. Slide motions of both the kinds, similarly to creep motions, consist in restructuring processes of chevron smectic layers into bookshelf layers, or conversely. Since these processes have strongly noncollective character at high voltages, the creep-to-slide dynamic

transition is not reflected in the electro-optic response spectra of SSFLCs. It has been shown that depending on the frequency of the driving voltage, the switching phenomena (at very high voltages) rely on the propagation of solitary waves or on complete switching (of the entire sample polarization) during each voltage cycle. Consequently, the mechanism of the transition between sliding and switching dynamic modes is, in general, different in different frequency regimes. Results presented in this paper show that, in spite of obvious analogies, dynamic phases, and transitions between them have essentially different character in cases of SSFLCs and ferroics.

ACKNOWLEDGMENTS

This work was supported by the funds for science in years 2007–2010 as a research project.

*jezewski@ifmpan.poznan.pl

- ¹I. Chuang, R. Durrer, N. Turok, and B. Yurke, *Science* **251**, 1336 (1991).
- ²P. C. Willis, N. A. Clark, J.-Z. Xue, and C. R. Safinya, *Liq. Cryst.* **12**, 891 (1992).
- ³S. T. Lagerwall, *Ferroelectric and Antiferroelectric Liquid Crystals* (Wiley-VCH, Weinheim, 1999), Chap. 8.
- ⁴P. Chauve, T. Giamarchi, and P. Le Doussal, *Phys. Rev. B* **62**, 6241 (2000).
- ⁵A. Vella, R. Intartaglia, C. Blanc, I. I. Smalyukh, O. D. Lavrentovich, and M. Nobili, *Phys. Rev. E* **71**, 061705 (2005).
- ⁶W. Kleemann, *Annu. Rev. Mater. Res.* **37**, 415 (2007).
- ⁷D. A. Allwood, G. Xiong, C. C. Faulkner, D. Atkinson, D. Petit, and R. P. Cowburn, *Science* **309**, 1688 (2005).
- ⁸B. B. Van Aken, J.-P. Rivera, H. Schmid, and M. Fiebig, *Nature (London)* **449**, 702 (2007).
- ⁹Y.-H. Shin, I. Grinberg, I.-W. Chen, and A. M. Rappe, *Nature (London)* **449**, 881 (2007).
- ¹⁰J. E. García, R. Pérez, D. A. Ochoa, A. Albareda, M. H. Lente, and J. A. Eiras, *J. Appl. Phys.* **103**, 054108 (2008).
- ¹¹A. Glatz, T. Nattermann, and V. Pokrovsky, *Phys. Rev. Lett.* **90**, 047201 (2003).
- ¹²Th. Braun, W. Kleemann, J. Dec, and P. A. Thomas, *Phys. Rev. Lett.* **94**, 117601 (2005).
- ¹³P. J. Metaxas, J. P. Jamet, A. Mougin, M. Cormier, J. Ferré, V. Baltz, B. Rodmacq, B. Dieny, and R. L. Stamps, *Phys. Rev. Lett.* **99**, 217208 (2007).
- ¹⁴W. Kleemann, J. Rhensius, O. Petravic, J. Ferré, J. P. Jamet, and H. Bernas, *Phys. Rev. Lett.* **99**, 097203 (2007).
- ¹⁵W. Kleemann, J. Dec, S. A. Prosandeev, T. Braun, and P. A. Thomas, *Ferroelectrics* **334**, 3 (2006).
- ¹⁶N. A. Clark and S. T. Lagerwall, *Appl. Phys. Lett.* **36**, 899 (1980).
- ¹⁷N. A. Clark and T. P. Rieker, *Phys. Rev. A* **37**, 1053 (1988).
- ¹⁸Geometry of the chevron structured smectic layers in SSFLCs and the structure of zigzag walls is detailed described in Refs. **3** and **17**; see also Refs. **19** and **20**.
- ¹⁹W. Jeżewski, W. Kuczyński, and J. Hoffmann, *Phys. Rev. E* **73**, 061702 (2006).
- ²⁰W. Jeżewski, W. Kuczyński, and J. Hoffmann, *Phys. Rev. B* **77**, 094101 (2008).
- ²¹W. Jeżewski, W. Kuczyński, and J. Hoffmann, *Liq. Cryst.* **34**, 1299 (2007).
- ²²G. Por and A. Buka, *J. Phys. (France)* **50**, 783 (1989); A. Jákli, N. Éber, and L. Bata, *Ferroelectrics* **113**, 305 (1991); A. Jákli, *Mol. Cryst. Liq. Cryst. (Phila. Pa.)* **292**, 293 (1997).
- ²³M. A. Handschy, N. A. Clark, and S. T. Lagerwall, *Phys. Rev. Lett.* **51**, 471 (1983).
- ²⁴J. E. Maclennan, M. A. Handschy, and N. A. Clark, *Liq. Cryst.* **7**, 787 (1990).
- ²⁵W. Jeżewski, W. Kuczyński, J. Hoffmann, and D. Dardas, *Opto-Electron. Rev.* **16**, 281 (2008).
- ²⁶W. Kuczyński, in *Dielectric Properties of Liquid Crystals*, edited by Z. Galewski and L. Sobczyk (Transworld Research Network, Trivandrum, 2007).
- ²⁷J. F. Li, X.-Y. Wang, E. Kangas, P. L. Taylor, C. Rosenblatt, Y. I. Suzuki, and P. E. Cladis, *Phys. Rev. B* **52**, R13075 (1995).
- ²⁸J. E. Maclennan, N. A. Clark, M. A. Handschy, and M. R. Meadows, *Liq. Cryst.* **7**, 753 (1990); J. Xue and N. A. Clark, *Phys. Rev. E* **48**, 2043 (1993).
- ²⁹K. H. Yang, T. C. Chieu, and S. Osofsky, *Appl. Phys. Lett.* **55**, 125 (1989).
- ³⁰S. A. Pikin, in *Relaxation Phenomena, Liquid Crystals, Magnetic Systems, Polymers, T_c-Superconductors, Metallic Glasses*, edited by W. Hasse and S. Wróbel (Springer, New York, 2003).
- ³¹J.-K. Song, M. J. Sufin, and J. K. Vij, *Appl. Phys. Lett.* **92**, 083510 (2008).
- ³²M. Škarabot, I. Muševič, and R. Blinc, *Phys. Rev. E* **57**, 6725 (1998).
- ³³A. Becker, S. Ried, R. Stannarius, and H. Stegemayer, *Europhys. Lett.* **39**, 257 (1997); C. Langer and R. Stannarius, *Phys. Rev. E* **58**, 650 (1998); C. Langer and R. Stannarius, *Ferroelectrics* **244**, 347 (2000).